THE JOURNAL OF PHYSICAL CHEMISTRY C

Article

pubs.acs.org/JPCC

Inhibition of 2,4-Dichlorophenoxyacetic Acid to Catalase Immobilized on Hierarchical Porous Calcium Phosphate: Kinetic Aspect and Electrochemical Biosensor Construction

Fengping Liu,[†] Aiming Zhong,[‡] Qin Xu,*[,†] Hongen Cao,[†] and Xiaoya Hu*[,†]

[†]College of Chemistry and Chemical Engineering, Yangzhou University, Yangzhou 225002, China

[‡]Yangzhou Polytechnic Institute, Yangzhou, 225127, China

Supporting Information

ABSTRACT: The inhibition mechanism of 2,4-dichlorophenoxyacetic acid (2,4-D) to catalase was studied by a catalase biosensor in a flow-injection analysis (FIA) system. This system provides an ideal sensing platform to electrochemically evaluate the chemical mechanism of enzyme inhibition. Hierarchical porous calcium phosphate (hp-CaP), as a biocompatible nanomaterial, was used to immobilize catalase for repeat use. 2,4-D together with H_2O_2 was injected into the bioreactor of the immobilized catalase-FIA system during the experimental procedure. The activity of the immobilized catalase was inhibited, which caused a decrease of the catalase-catalyzed H_2O_2 reduction current. Lineweaver−Burk, Dixon, and Cornish−Bowden plots confirmed that the inhibition of catalase by 2,4-D followed an competitive mechanism with a inhibition constant of 4.78×10^{-7} M. Based on this inhibition characters, a biosensor for 2,4-D detection was constructed. This biosensor showed a linear range from 0.03 to 3.00 μM with a detection limit of 0.015 μM. It demonstrated good stability, acceptable reproducibility and low cost for 2,4-D screening. It has been successfully applied for the determination of 2,4-D in commercial bean sprouts samples. It is anticipated that a rapid evaluation of the chemical mechanism of catalase inhibition by the FIA system could pave the way to rationally designing biosensors.

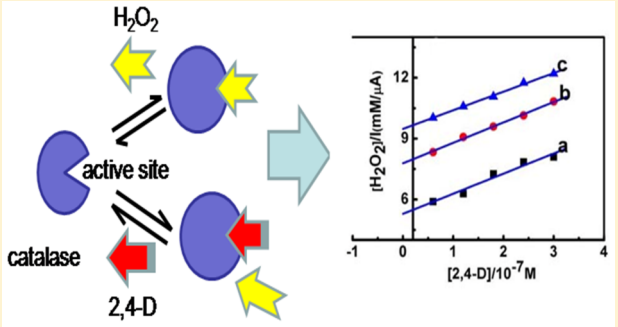

INTRODUCTION

Catalase, as one of the most important components of the antioxidant systems, serves to protect cells from the toxic effects of reactive oxygen species (ROS) by catalyzing hydrogen peroxide decomposition into molecular oxygen and water without producing free radicals.[1] The importance of catalase in scavenging ROS generated under stress conditions has been proven by Willekens et al.[2] A decrease of the activity of catalase is frequently observed under some stress conditions[3] or in the presence of inhibitors.[4] Understanding the physical and functional interactions between molecules and catalase is of vital importance in biology and physical chemistry. Furthermore, the careful investigation of the type and mechanism of inhibition would help to rationally design biosensors based on the inhibition principles.[5]

2,4-Dichlorophenoxyacetic acid (2,4-D) is a phenoxy herbicide that has been widely used for postemergence control of annual and perennial broad-leaved weeds.[6] It is also an active ingredient of more than 1000 pesticides. Unfortunately, the improper use of 2,4-D would cause serious threats to human health even at trace levels[7] and may lead to the overproduction of reactive oxygen species (ROS).[8] Previous studies have shown that 2,4-D can act as a potent inhibitor for the activity of catalase in wheat and other plant species.[9] Despite the interest in studying the effect of 2,4-D to catalase in plants, many fundamental questions regarding the mechanisms responsible for the observed effects of 2,4-D to catalase remain unanswered. The studying of the chemical mechanism between 2,4-D and catalase and how these interactions influence their biological functions would help us guide the proper use of 2,4-D. Furthermore, the inhibition mechanism study would also help to rationally design a kind of inhibition biosensor for 2,4-D detection.[10]

So far, a variety of analytical techniques have been developed for the characterization and identification of the interaction between catalase and small molecules or nanoparticles.[11] However, most of these methods suffer from high cost, low sensitivity, and complex procedure. As an alternative, the electrochemical approach attracts appreciable attention because of its inherent specificity, high sensitivity, simplicity, and low cost. It has been applied to investigate the interaction between proteins and nanoparticles[12] or organic compounds.[13] On the basis of the numerous studies reported before, the kinetics of

Special Issue: Kohei Uosaki Festschrift

Received: December 23, 2015
Revised: March 15, 2016
Published: March 16, 2016

DOI: 10.1021/acs.jpcc.5b12559
J. Phys. Chem. C 2016, 120, 15966−15975

Scheme 1. Scheme of the Amperometric Flow Injection (FIA) System for Inhibition Study and 2,4-D Detection

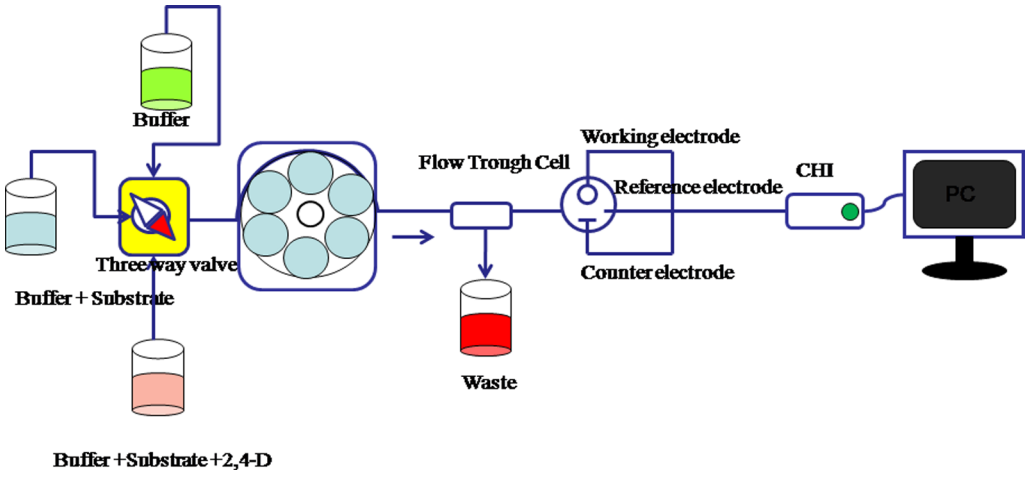

the enzyme inhibition depends strongly on the immobilization of enzymes.[14] The immobilization of enzymes on different materials increases their stability,[15] reduces the time of analysis and make the enzymes suitable in flow systems for repetitive analyses. Different kinds of nanomaterials have been used for the immobilization of enzymes.[16] Calcium phosphate is a biocompatible material with unique physicochemical properties, such as biocompatible, osteoconductive, nontoxic, noninflammatory, nonimmunogenic, and bioactive.[17] It has been primarily used as bone substitutes. Due to its ability to bind proteins by multiple-site without denaturing them, it has also been used as carriers for peptides, for protein immobilization or DNA delivery.[18] Furthermore, CaP shows good performance for the construction of electrochemical biosensors because Ca^{2+} and PO_4^{3-} can be used as promoters to facilitate electron transfer of proteins.[19] In this work, hierarchical CaP containing bimodal interconnected macroporous and mesoporous structures was used as the matrix for proteins immobilization and biosensor construction owing to its high surface area and advantages in mass transport.[20]

Here we described an electrochemical flow injection (FIA) system coupled with a electrochemical detector to study the interaction between 2,4-D and catalase immobilized on hierarchical porous calcium phosphate (hp-CaP) (Scheme 1). hp-CaP, as a biocompatible material, was applied for the immobilization of catalase to improve the stability of catalase for repeat use. Chitosan is a natural-biopolymer with abundant amino groups. In this work, it was used to help the stable dispersion of hp-CaP in aqueous solution and to provide a good biocompatible microenvironment for sensors construction because of its good biocompatibility and excellent film-forming ability.[21] This system has been employed as a sensing platform to study inhibition mechanism of 2,4-D to the immobilized catalase and for 2,4-D screening.

EXPERIMENTAL SECTION

Reagents and Apparatus. Bovine liver catalase (E.C. 1.11.1.6) was obtained from Sigma and was used without further purification. Chitosan and hydrogen peroxide (H_2O_2) (30%) were bought from Shanghai Chemical Reagent Co. (Shanghai, China). 2,4-D was purchased from Chem Service (American). Prometryn, clethodim, cycloxydim, sethoxydim, 2,4-dichlorophenylacetic acid, and 2,4-dichlorobenzoic acid were all purchased from Aladdin Reagent Company. The standard 2,4-D stock solution (3.0 mM) was prepared in anhydrous ethanol. Working solutions of 2,4-D were obtained by serial dilution of the stock solution with 0.1 M phosphate buffer solution. The bean sprouts were bought from local markets. All other reagents not mentioned here were of analytical-reagent grade and were used without further purification. Doubly distilled water was used throughout the experiment. Phosphate buffer solution was prepared by mixing 0.1 M Na_2HPO_4 and 0.1 M NaH_2PO_4 and then adjusted to the desired pH by NaOH or H_3PO_4.

The morphologies of hp-CaP and catalase/hp-CaP were investigated by using a Zeiss Supra55 field emission scanning electron microscope (Zeiss Supra, Germany) and a JEM-2100 transmission electron microscope (Japan) using an accelerating voltage of 200 kV. The Fourier transform infrared (FT-IR) spectra were measured on a FT-IR Spectrophotometer (IFS66/S, Bruker, USA). All the electrochemical measurements were carried out on a CHI 840B electrochemical analyzer (Shanghai Chenhua, China) using a conventional three-electrode system. In this system, a platinum coil acted as the counter electrode, a commercial Ag/AgCl (saturated KCl) as the reference electrode, and bare or modified glassy carbon electrodes (GCEs) (Wuhan Gaossunion, China) as working electrodes. Before use, the GCEs were polished with 0.05 μm alumina slurry and rinsed with doubly distilled water. The flow injection system was composed of a peristaltic pump coupled to a multiport valve (Ismatec ISM 828) and an electrochemical flow-through cell (Chenhua, Shanghai).

Preparation of hp-CaP and Fabrication of Catalase/hp-CaP Modified Electrode. The hp-CaP was prepared according to our previous reported work[22] with a minor modification. The pollen grains (5.0 g) were cleaned by 50 mL of ethanol under ultrasonication for 1 h, and then they were added into a 50 mL mixture containing alcohol and formaldehyde (1:1 in volume) under vigorous stirring for 10 min to fix the morphology. Finally, the grains were washed with distilled water and dried at 80 °C for 6 h. hp-CaP were produced by soaking 0.5 g of the pretreated grains in 5 mL of 0.1 M $CaCl_2$ and Na_2HPO_4 (5 mL, 0.1 M, pH 9.04) for 24 h, respectively. The precipitate was washed, and was sealed into a 100 mL Teflon-lined autoclave, heated to 400 °C, and maintained at this temperature for 10 h. After the autoclave had cooled down to room temperature naturally, the products were collected and washed with deionized water. The as-

DOI: 10.1021/acs.jpcc.5b12559
J. Phys. Chem. C 2016, 120, 15966−15975

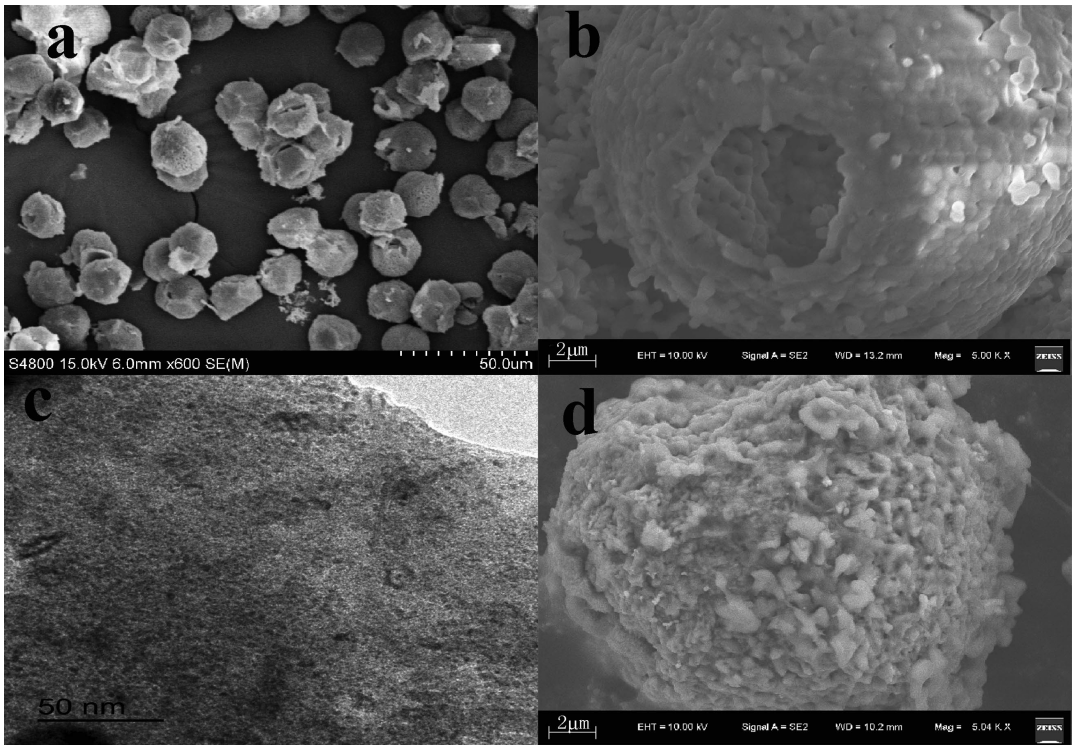

Figure 1. SEM (a and b) and TEM (c) images of hp-CaP; d corresponds to the SEM image of catalase/hp-CaP.

prepared sample was then heated at 600 °C for 5 h to produce hp-CaP.

For catalase/hp-CaP modified electrode, different amounts of hp-CaP were dispersed in 1.0 mL of 0.5% chitosan solution (CS) homogeneously with ultrasonication. Then 50.0 μL of 8.0 mg/mL of catalase solution was added into 50.0 μL of the well-dispersed hp-CaP solution. The mixture was shaken strongly for about 30 min at room temperature for the adsorption of catalase. For electrode modification, 5.0 μL of the above obtained mixture was spread evenly onto the pretreated glassy carbon electrode by a syringe. The electrode was left to dry at 4 °C. The resulting electrode was marked as catalase/hp-CaP. When not in use, the modified electrodes were stored at 4 °C.

Electrochemical Experimental Procedures. All the cyclic voltammetric (CV) measurements were performed in 10.0 mL of the N_2-saturated phosphate buffered solution (0.1 M, pH 7.0). The electrochemical impedance spectroscopy (EIS) measurement was recorded in 0.1 M phosphate buffer (pH 7.0) containing 0.1 M KCl and 5 mM $K_3Fe(CN)_6$/$K_4Fe(CN)_6$ with a frequency range from 0.01 to 1.0×10^5 Hz. FIA measurements with amperometric detection were carried out at an applied potential of −350 mV versus Ag/AgCl. The carrier stream was 0.1 M phosphate buffer (pH 7.0) with a flow rate of 3 mL/min. The sample injection volume was of 50 μL.

For the determination of Michaelis constant (K_m), maximum velocity (V_{max}) values of the catalase immobilized on hp-CaP, and the inhibition type, catalase activities were measured with H_2O_2 at varying concentrations by using an amperometric method. Different concentrations of hydrogen peroxide were passed through the catalase/hp-CaP/GCE, and the reduction currents of H_2O_2 on this electrode were recorded. Kinetic constants (V_{max} and K_m values) were calculated from the slopes and intercepts of the Lineweaver−Burk plots.[23] Inhibition type and constant were obtained from Dixon plots and Cornish-Bowden plots. For the determination of 2,4-D, the solutions containing different amounts of 2,4-D with the fixed amount of H_2O_2 were passed through the catalase/hp-CaP/GCE by the FIA system. The inhibition percentage (Inh%) at each 2,4-D concentration was calculated using the expression shown below (eq 1):

$$\text{Inh\%} = \frac{(I_0 - I)}{I_0} \times 100\% \quad (1)$$

where I_0 and I are the currents of the biosensor obtained in absence and presence of 2,4-D, respectively. The resulting Inh% can be plotted versus molar inhibitor concentration to create a 2,4-D assay.

RESULTS AND DISCUSSION

Characterization of hp-CaP, Catalase, and Catalase/hp-CaP. The porous networks and morphology of the hp-CaP and catalase/hp-CaP can be directly observed from SEM and TEM images. SEM images (Figure1a,b) reveal that the as-prepared hp-CaP are spheres with diameters of 5−6 μm. These spheres, constructed by nanoparticles, possess a three-dimensional interconnecting porous structure. Numerous of nano-scaled cavities with the diameter about 250 nm are existed on the surface of the hp-CaP microspheres (Figure 1b). TEM image shows that these nanoparticle units contain numerous micropores about 2−3 nm, and their compact and loose aggregation leads to mesopores and macropores, respectively (Figure 1 c). These porous structures can greatly enhance the active surface area available for protein binding. Meanwhile, the pores on hp-CaP will provide convenience for the substrate to access the immobilized protein. Little changes on the morphology of hp-CaP occur after the immobilization of catalase except the presence of some aggregates on the surface (Figure 1d). These aggregates are the immobilized catalase. Catalase sequestered into the cavities or bind on the surface of

DOI: 10.1021/acs.jpcc.5b12559
J. Phys. Chem. C 2016, 120, 15966−15975

hp-CaP microspheres. The cavities on hp-CaP may provide a protective microenvironment for catalase to retain its stability and activity by limiting the conformational change and unfolding of the entrapped catalase.

FT-IR is a sensitive technique to monitor the structure change of proteins. A protein's FTIR spectrum has two prominent features, the Amide I (~1650 cm^{-1}) and Amide II (~1540 cm^{-1}) bands, where the former arise primarily from the C = O stretching vibration and the latter is attributed to the N−H bending and C = N stretching vibrations of the peptide backbone.[24] The absorption bands at 1525 and 1625 cm^{-1}, which are attributed to amide II and amide I bands, can be seen in catalase (Figure 2 b) and catalase/hp-CaP (Figure 2c) but

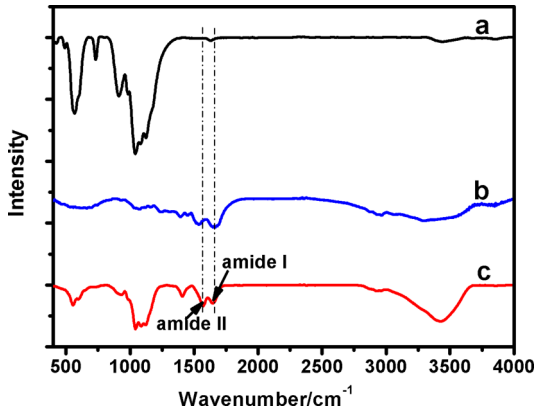

Figure 2. FT-IR spectra of hp-CaP (curve a), catalase (curve b), and catalase/hp-CaP (curve c).

cannot be seen in hp-CaP (Figure 2 a). This proves that catalase has been immobilized on hp-CaP. Almost no changes on the amide bands of catalase are observed after the immobilization process, implying that most of catalase preserved their native structure after being adsorbed on the hp-CaP.

Electrochemical Behavior of Catalase/hp-CaP/GCE. Figure 3 compares the CV and EIS responses of different electrodes. The bare GCE (curve a, Figure 3A) and hp-CaP/GCE (curve b, Figure 3A) do not show any apparent redox waves in the studied potential range. In contrast, catalase/hp-CaP/GCE (curve c, Figure 3A) exhibits a pair of well-defined redox peaks with a formal potential of about −0.25 V. The peak to peak separation is about 110 mV at the scan rate of 100 mV/s, suggesting fast electron transfer. Therefore, it can be concluded that catalase immobilized on hp-CaP underwent direct electron transfer between the active center of catalase and the electrode surface, and the observed redox peaks can be attributed to the redox reaction of the CAT-Fe(III)/CAT-Fe(IV) redox couple at the active site of the immobilized catalase.[25]

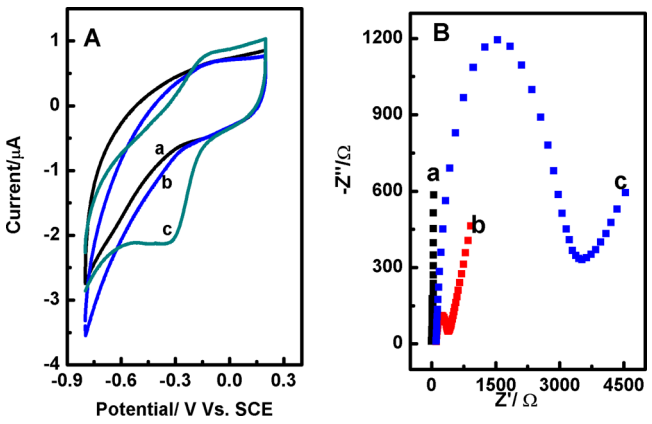

Figure 3. (A) CVs of the bare GCE (a), hp-CaP/GCE (b) and catalase/hp-CaP/GCE (c) in N_2-saturated phosphate buffer (pH 7.0, 0.1M) at the scan rate of 100 mV/s; (B) EIS of the bare GCE (a), hp-CaP/GCE (b) and catalase/hp-CaP/GCE (c) in 0.1 M phosphate buffer (pH 7.0) containing 0.1 M KCl and 5 mM $K_3Fe(CN)_6$/$K_4Fe(CN)_6$.

EIS is a powerful tool to characterize the modified electrodes. The semicircle portion at higher frequencies in the impedance spectrum corresponds to the electron transfer-limiting process, while the linear part at the low frequencies results from the diffusion-limiting step of the electrochemical process. The immobilization of substances, e.g. enzymes, antigens/antibodies or nanomaterials on electrodes always alters the interfacial capacitance and electron-transfer resistance of the conductive electrodes. The diameter corresponding to the electron transfer resistance (Ret) can be used to describe this alternation.[26] In Figure 3 B, the Ret of the bare GCE is approximately 382 Ω (curve a). With the immobilization of hp-CaP, the Ret of curve b increased to 586 Ω (curve b). The little increase of R_{et} between the bare GCE and the hp-CaP/GCE reflects that the modification of hp-CaP does not essentially affect the interfacial electron transfer. The conductivity of hp-CaP may be due to the ionic transport.[27] Furthermore, hp-Cap with large surface area and abundant adsorbing sites can provide a favorable electrochemical interface that would be beneficial to the construction of an electrochemical biosensor. The increase in interfacial transfer resistance is observed with a Ret of 2422 Ω (curve c) after catalase immobilized onto the hp-Cap/GCE. The remarkable increment of electron transfer resistance indicates that the electron transfer of $[Fe(CN)_6]^{3-/4-}$ was blocked further because of the insulation of catalase.

Inhibition Mode of 2,4-D to the Immobilized Catalase. The cyclic voltammograms of catalase/hp-CaP/GCE under different conditions were studied to check its applicability for studying the interaction between 2,4-D and the immobilized catalase. Figure 4A shows that the reduction current of catalase/hp-CaP/GCE at around −0.4 V is remarkably enlarged in the presence of 1.0 mM H_2O_2 (curve d). This observation clearly indicates that catalase immobilized on hp-CaP exhibited excellent bioelectrocatalytic activity for the reduction of H_2O_2 based on its direct electrochemistry.[28] The current obtained is proportional to the activity of catalase. The inset of Figure 4A compares the CV responses of catalase/GCE and catalase/hp-CaP/GCE in the absence and presence of the same concentration H_2O_2. The catalytic reduction current of H_2O_2 at the catalase/hp-CaP/GCE (curve b′) is higher than that at the catalase/GCE (curve a′). It means that the catalase/hp-CaP/GCE has a higher sensitivity for the detection of H_2O_2 than catalase/GCE. To evaluate the effect of 2,4-D on the enzymatic activity of the biosensor, measurements were performed by injecting different concentrations of 2,4-D into the solution with the fixed concentration of H_2O_2 (curve b and c in Figure 4A). With the increase of the introduced concentration of 2,4-D, the bioelectrocatalytic cathodic currents of catalase/hp-CaP/GCE decreased, indicating the inhibition effect of 2,4-D on the activity of catalase.

DOI: 10.1021/acs.jpcc.5b12559
J. Phys. Chem. C 2016, 120, 15966−15975

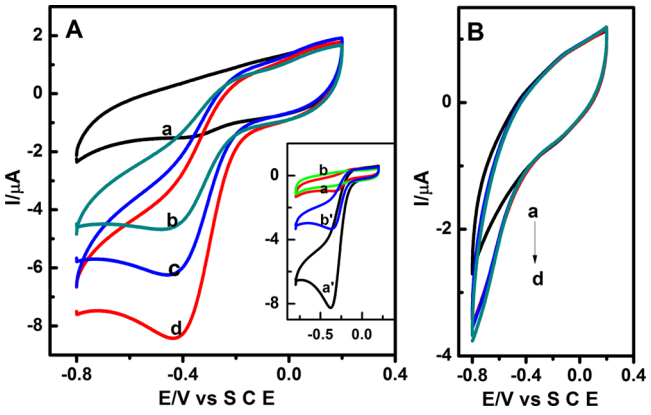

Figure 4. CVs of catalase/hp-CaP/GCE (A) hp-CaP/GCE(B) in N_2-saturated phosphate buffered solution (pH 7.0, 0.1 M) in the absence (curve a) and presence of 1.0 mM H_2O_2 (curve d). For curve c and curve b, the same as d except that 1.0 μM (c) and 2.0 μM (d) of 2,4-D presented. Scan rate: 100 mV/s. Inset of panel A is the CV responses of catalase/hp-CaP/GCE (curves a and a′) and catalase/GCE (curves b and b′) in the absence (curves a and b) and presence of 1.0 mM H_2O_2 (curves a′ and b′).

The cyclic voltammograms of H_2O_2 at the hp-CaP/GCE was also investigated. It is evident that the voltammograms of hp-CaP/GCE differed substantially from that of the catalase/hp-CaP/GCE in the absence and presence of H_2O_2 (Figure 4B). There was no obvious peak corresponding to the reduction or oxidation of H_2O_2 within the studied potential window (curve d, Figure 4B). This is in line with the results reported by Lei et al.,[29] where little reduction peak for hydrogen peroxide was seen at a bare glassy carbon electrode. When 2,4-D was added into the solution containing H_2O_2 (curve c and b in Figure 4B), almost no reduction of the current was observed. Thus, it is reasonable to say that the observed decrease of the cathodic currents of catalase/hp-CaP/GCE in the presence of 2,4-D is caused by the inactivation of the catalytic activity of catalase for H_2O_2 reduction. The binding of 2,4-D inhibits the reaction between H_2O_2 and catalase, resulting in the change of the CV responses. The concentration of 2,4-D can be estimated by comparing the differences in the limiting currents obtained.

It is essential to evaluate the inhibitory mechanism in order to determine the suitability of the catalase/hp-CaP/GCE for a screening assay.[30] Michaelis−Menten analysis was used to study the electrocatalytic reduction of H_2O_2 by catalase/hp-CaP/GCE with and without 2,4-D present. When catalytic activity follows Michaelis−Menten kinetics over the range of substrate concentrations tested, the kinetic constants Km and inhibition type can be determined by Lineweaver−Burk plot (also known as the double-reciprocal plot).[23] Figure 5A shows the double-reciprocal Lineweaver−Burk plots of catalase/hp-CaP biosensor. The plots of $1/V$ versus $1/[S]$ gave a family of straight lines with different slopes, which intersected on the ordinate with a common intercept, indicating that 2,4-D is a competitive inhibitor to the immobilized catalase. Based on the Lineweaver−Burk equation, the K_m of catalase/hp-CaP/GCE and catalase/GCE were calculated to be 1.22 mM and 12.68 mM, respectively. Both of them are lower than the reported value of 25.2 mM of catalase in solution,[31] indicating that the immobilization procedure improves the affinity of catalase to H_2O_2. The large surface area and particular multiadsorbing sites of hp-CaP help the assembly and the orientation of catalase, which improved the affinity between H_2O_2 and catalase. The inhibitor constant, K_i, can be calculated from the Michaelis equation or by using Figure 5 A to draw a secondary plot. However, the Lineweaver−Burk plot provides the worst estimation of the kinetic constants because of the crowding of high-substrate concentration data points close to the ordinate axis. Slope and intercept reploting cause a further magnification of errors in determining kinetic parameters.[32]

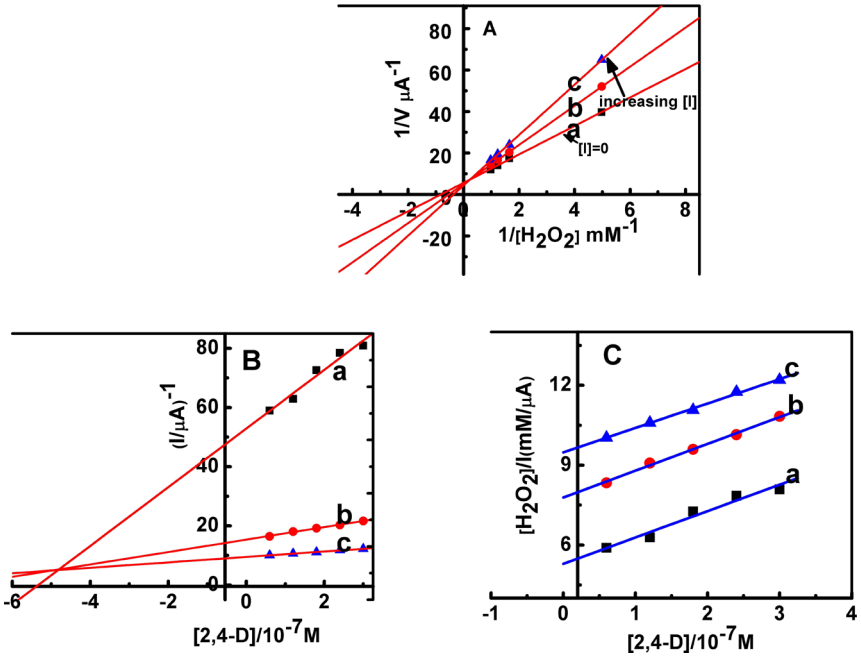

Figure 5. Type of 2,4-D inhibition to catalase immobilized on hp-CaP as inferred from the (A) Double-reciprocal Lineweaver−Burk plot; (B) Dixon plot and (C) Cornish-Bowden plot. The Lineweaver−Burk plot was obtained in the absence (a) and presence of 3.0 μM (b) and 6.0 μM 2,4-D (c), but the Dixon and Cornish-Bowden plots were obtained in the presence of 0.1 mM (a), 0.5 mM (b) and 1.0 mM (c) H_2O_2, respectively.

DOI: 10.1021/acs.jpcc.5b12559
J. Phys. Chem. C 2016, 120, 15966−15975

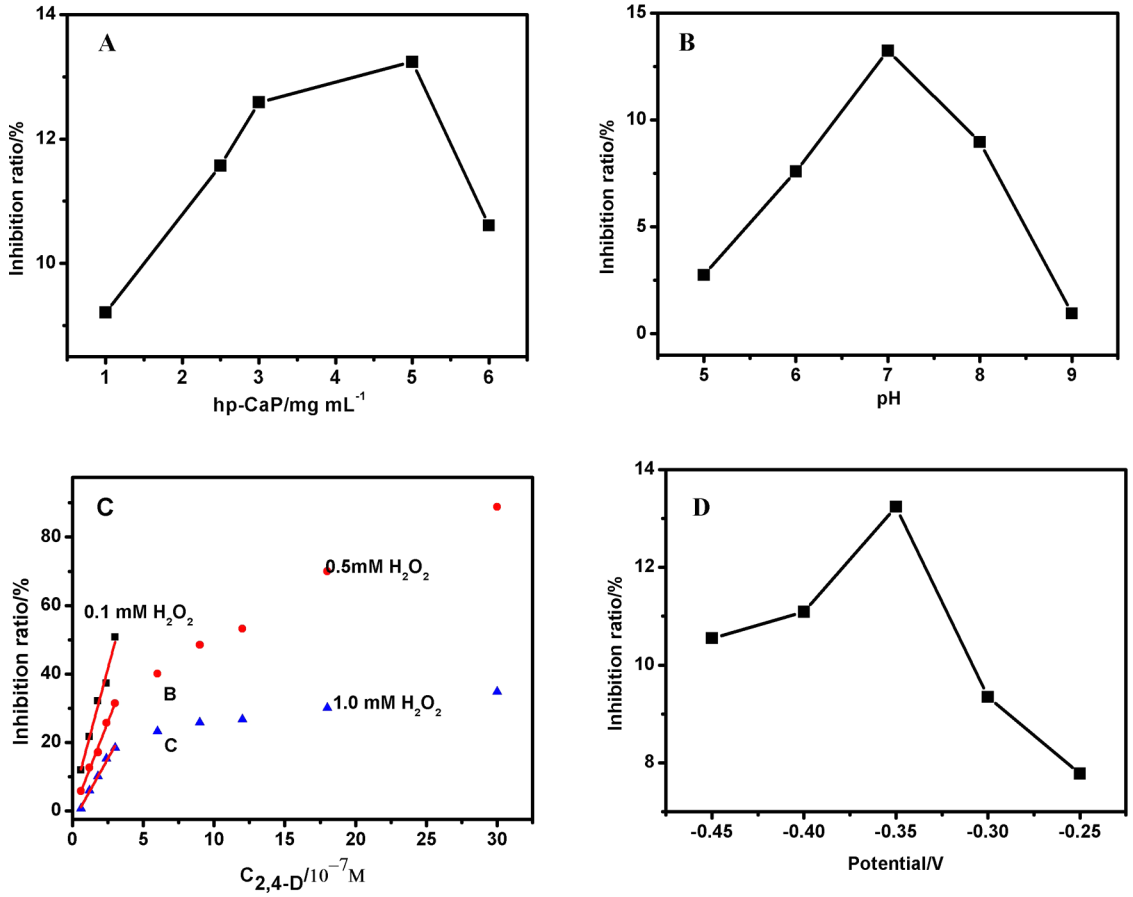

Figure 6. (A) Influence of hp-CaP amount on the inhibition of catalase/hp-CaP biosensor in pH 7.0 phosphate buffered solution by 0.1 μM 2,4-D; (B) Influence of pH on the inhibition of catalase/hp-CaP biosensor under different pH by 0.1 μM 2.4-D; (C) Influence of the H_2O_2 concentration on the sensitivity and linear range of catalase/hp-CaP biosensor for 2,4-D; D) Influence of the applied potential on the inhibition degree of catalase/hp-CaP biosensor by 0.1 μM 2,4-D in pH 7.0 phosphate buffered solution.

The Dixon plot[33] and Cornish-Bowden plot[34] are frequently used for both identification of the likely mechanism of enzyme inhibition and for estimation of the inhibitory constant K_i. Dixon Plots of the reciprocal of the rate of product formation $(1/V)$ versus inhibitor concentration [I] at each substrate concentration [S] were prepared. For each [S] value, the points lie on a straight line, and the extrapolated lines at different [S] values intersect at a single point, for which [I] = $-K_i$. The best part of the Dixon and Cornish−Bowden methods is that there are really no calculations to be done. The inhibition constant can be obtained directly from the plots. Figure 5B shows the Dixon plot for the inhibition of the immobilized catalase. The resulting linear curves converges in the upper left quadrant of the plot, demonstrating that 2,4-D is a competitive or mixed inhibitor. However, the usefulness of this method is limited by the fact that it does not distinguish unambiguously between competitive and mixed inhibitors, and, for mixed or uncompetitive inhibitors, it provides no measure of the dissociation constant of the EIS complex.[35] The Cornish−Bowden plot is similar to the Dixon plot but complementary to it. This plot gives a relationship between [S]/V against [I]. It should provide good estimates of K_i, since the variance of [S]/V does not vary greatly with V if V is distributed with uniform variance. Figure 5C is a Cornish−Bowden plot. The lines are parallel in the plot of [S]/V against inhibitor concentration. The result further unambiguously indicated the competitive type of inhibition for 2,4-D. Scheme S1 gives the structure of 2,4-D and illustrates the inhibition mechanism. 2,4-D competes with H_2O_2 for the active site of catalase, and thus causes the activity decrease of catalase. The inhibitor constants (K_i) was calculated as 4.78×10^{-7} M. The apparent inhibition constant is a measure of the sensor's efficiency in detecting the inhibitor. The lower the apparent inhibition constant, the higher the sensor efficiency in detecting the respective inhibitor.[36] The inhibition mechanism and the low inhibition constant of 2,4-D to the immobilized catalase indicated that a sensitive inhibition biosensor can be constructed for 2,4-D detection based on the catalase/hp-CaP/GCE.

Optimization of the Variables Concerning the Catalase/hp-CaP Biosensor under Flow-Injection Conditions. To obtain good performance of catalase/hp-CaP biosensor for 2,4-D detection, several experimental parameters including the amount of hp-CaP, pH, the concentration of H_2O_2, and the applied potential were optimized. The dependence of inhibition rate on the amount of hp-CaP is shown in Figure 6A. As can be seen, the inhibition rate increased evidently as the amount of hp-CaP increased from 1.0 mg/mL to 5.0 mg/mL. The maximum inhibition degree was obtained when 5.0 mg/mL of hp-CaP was used for the immobilization of 8.0 mg/mL of catalase. This optimized mass amount of hp-CaP was applied in all the following experiments.

In amperometric measurement, a crucial parameter is the operating potential. In the present study, the dependence of the inhibition ratio on the applied potential was investigated

DOI: 10.1021/acs.jpcc.5b12559
J. Phys. Chem. C 2016, 120, 15966−15975

(Figure 6B). The inhibition ratio increased with the operating potential between −0.25 and −0.35 V, and then decreased. A maximum inhibition ratio was observed at −0.35 V. This can be due to a potential dependence of the activity of the immobilized catalase. −0.35 V was used as the detection potential for further studies.

Another important aspect to be investigated concerns the concentration of substrate (H_2O_2). For competitive inhibition, the inhibition is most noticeable at low substrate concentrations but can be overcome at sufficiently high substrate concentrations. However, increasing the concentration of substrate provides the largest signal-to-background ratio that can be obtained for an assay.[37] In order to study this effect, assays were performed using different concentrations of H_2O_2 in the measuring cell. These concentrations lay in the linear range of the calibration plot for H_2O_2 with the catalase/hp-CaP biosensor; therefore the decrease in current due to the presence of 2,4-D could be directly correlated with the activity inhibition of 2,4-D, making it possible to assess the presence of 2,4-D. The results indicate that the lower the concentration of hydrogen peroxide, the greater the inhibition ratio observed (Figure 6C). For 0.1 mM H_2O_2, a sensitivity of 15.51 ± 2% was obtained, whereas 10.72 ± 1.7% and 7.1 ± 1.4% were obtained for 0.5 and 1.0 mM H_2O_2, respectively. However, low reduction current of H_2O_2 on catalase/hp-CaP biosensor gave rise to a lower signal-to-noise ratio, and the linear range is narrow. When the concentration of H_2O_2 was 1.0 mM, there was a higher probability of H_2O_2 occupying the active site over the 2,4-D at a fixed concentration. Therefore, increasing the concentration of H_2O_2 decreases the ability of competitive 2,4-D to bind and inhibit catalase, thus decreased the sensitivity of the sensor. Considering the sensitivity and linear range, 0.5 mM H_2O_2 was chosen for further studies

The inhibition response of catalase/hp-CaP biosensor in the electrochemical cell containing working solutions of different pH values was also evaluated in order to determine the optimum pH value for 2,4-D detection. Figure 6 D shows that a maximum inhibition response for catalase/hp-CaP biosensor was observed at pH 7.0, which is similar to previously reported work.[38] Catalase operates best within a specific pH range, and would be denatured by excessive acidity or alkalinity. Therefore, a pH value of 7.0 was selected for 2,4-D detection with the catalase/hp-CaP biosensor system.

Performance Characteristics of the Catalase/hp-CaP Biosensor. Since the FIA method has several advantages such as good reproducibility, good stability and high sample throughput,[39] this method was used for the determination of 2,4-D by using catalase/hp-CaP as the sensor element. Figure 7 displays that the amperometric response of catalase/hp-CaP biosensor decreased stepwise with successive injection of different concentrations of 2,4-D in the presence of constant concentrations of H_2O_2. This signal decrease was attributed to the inhibition effect of 2,4-D to the activity of the immobilized catalase. Two linear ranges were obtained for this catalase/hp-CaP biosensor (inset of Figure 7). One is from 0.03 to 0.30 μM with a regression equation of Inh(%) = 3.33+ 1.08 × 10^8 C (M) (R^2 = 0.999, n = 6), and the other one is from 0.30 to 3.00 μM with a regression equation of Inh (%) = 31.63 + 2.07 × 10^7C (M) (R^2 = 0.996, n = 6), where C is the concentration of 2,4-D. The detection limit was 0.015 μM, considering 3% standard deviation and a signal-to-noise ratio of 3. This detection limit is below the maximum residue limits (MRLs) defined by the European Union (0.045 μM) and China (0.9 μM) for 2,4-D,

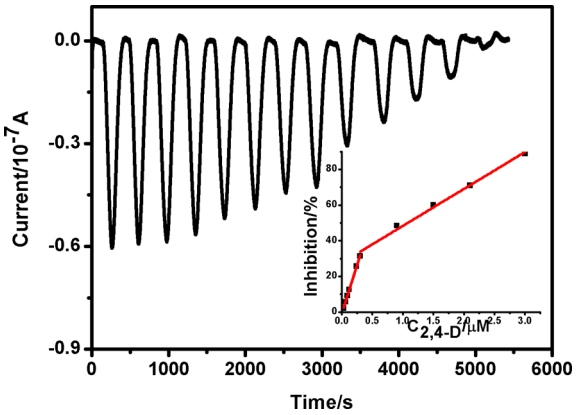

Figure 7. Flow-injection amperometric curves of catalase/hp-CaP biosensor for different concentrations of 2,4-D. Inset was the calibration curves between 2,4-D and inhibition efficiency. The experiment was performed in 0.1 M phosphate buffered solution (pH 7.0) containing 0.5 mM H_2O_2 at −0.35 V; the data represented mean values and standard deviations of six measurements.

suggesting the suitability of this sensor for screening of 2,4-D.[40] Several methods have been applied for the detection of 2,4-D, for example, high performance liquid chromatographic method,[41] immunoassays,[40] electrochemical methods[42] etc. Table 1 listed the analytical performance of different methods for 2,4-D detection. This biosensor is more sensitive than some of the reported work,[40−43] and highly comparable with the previously reported chemiluminescent enzyme-linked immunosorbent assay method.[44] Although immunoassays exhibit promising sensitivity, they often involved a monoclonal or a polyclonal antibody of antibody tagged with enzymes, fluorophores or nanomaterials. These approaches with complicated preparation and detection processes are often time-consuming, inconvenient, expensive, and labor-intensive. This inhibition method we provided is simple and low cost.

The influence of several possible interference species from plant samples on the determination of 2,4-D was studied under the optimum condition. A 0.1 μM standard solution of 2,4-D was examined both in the presence and absence of various interferences in the buffer solution using the biosensor. The inhibition ratio was normalized on the basis of the response under optimized conditions for 0.1 μM of 2,4-D. No influence was found after the addition of 1000-fold concentrations of glucose, sucrose, glycine, citric acid, Na^+, Ca^{2+}, and Mg^{2+}, 50-fold concentration of prometryn, clethodim, cycloxydim, sethoxydim, and 10-fold concentrations of Fe^{3+}, forchlorfenuron and salicylic acid. However, the compounds structurally similar to 2,4-D, namely 2,4-dichlorophenylaceticacid, 2,4-dichlorobenzoic acid, would cause the interferences when their concentrations were 0.3 μM. This may be attributed to the fact that the inhibition of catalase activity lacks specificity, which is also typical for other inhibition biosensors.[47] However, the developed inhibition biosensor is capable not only of detecting a single chemical species, but also of giving a global evaluation of the overall contamination of the sample by 2, 4-D and its analogues, which are endowed with the same toxicity. This biosensor can be applied for the preliminary screening of various contaminants in environmental or food matrices, possibly minimizing the pretreatment of samples, reducing the cost and time of analysis, and extending the number of sampling sites or of samples assayed per site. The exact composition and the chemical structure of all contaminants

DOI: 10.1021/acs.jpcc.5b12559
J. Phys. Chem. C 2016, 120, 15966−15975

Table 1. Comparison of the Analytical Performance of Different Methods for 2,4-D Detection

methods	calibration range (μM)	detection limit (nM)	ref
diffraction gratings based on MIP	600−2000		43a
electrochemical sensor	1.0−10.0	830.0	42
liquid chromatographic analysis		135.0	41
piezoelectric immunosensor	0.06−3.00	58.0	43c
chemiluminescence immunosensor		13.0	43b
PEC sensor based on MIP modified TiO2 nanotubes	0.5−13.0	10.0	45
ELISA	0.02−2.91	6.0	44
PEC sensor based on BiOI	4.52×10^{-4} to 4.0×10^{-2} and 0.09−4.0	0.18	46
catalase/hp-CaP biosensor	0.03−3.00	15.0	this work

MIP: molecularly imprinted polymer; PEC: photoelectrochemical; ELISA: enzyme-linked immunosorbent assay.

may be obtained by more specific and sophisticated confirmation methods, usually based on chromatographic-spectrometric techniques (primarily GC−MS and HPLC−MS).

The precision of the biosensor was checked with its repetitive measurements of 0.1 μM of 2,4-D. The relative standard deviation was 3.42% (n = 10). Reversibility of inhibition was evaluated by measuring the biosensor's responses to 0.5 mM H_2O_2 before and after the inhibition effect of 2,4-D at a concentration of 3.0 μM. Between each measurement, the biosensor was washed with phosphate buffer. As shown in Figure 8, the signal changes are fully reversible, and the

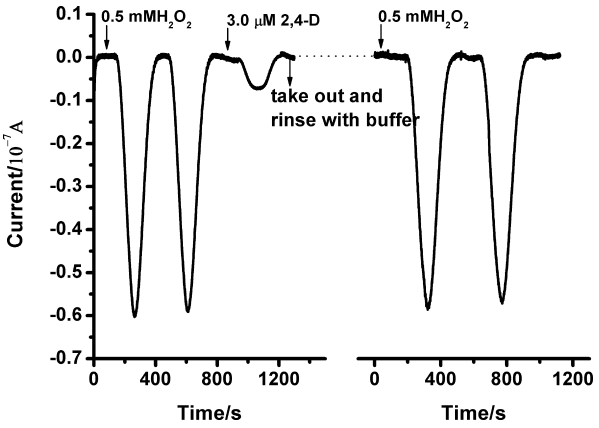

Figure 8. Reversibility test of the catalase/hp-CaP biosensor using 3.0 μM 2,4-D as the inhibitor.

biosensor can be repeatedly used for the detection of 2,4-D. The reproducibility of the biosensor was evaluated by the response variation of 10 batchs of catalase/hp-CaP, prepared on different days. The relative standard deviation was 8.72% (n = 10), indicating good reproducibility of the sensor. The stability of the biosensor was investigated by storing it at 4 °C in a refrigerator and checked its response to 0.1 μM of 2,4-D every day. The biosensor maintained 91.3% of its initial activity after one month. Thus, this biosensor has acceptable stability.

In order to validate the applicability, sensitivity, and accuracy of this catalase/hp-CaP biosensor for real samples analysis, a recovery experiment was carried out by adding the known amounts of 2,4-D into the extracted bean sprouts samples, and analyzed by using the described method under the optimal conditions. The recoveries of 2,4-D in the bean sprouts samples were in the range of 97.78−103.33%. Furthermore, the value of RSD is below 5.3%, demonstrating that this method is effective and applicatory.

CONCLUSIONS

The interaction between 2,4-D and catalase has been studied by a simple and effective biosensor with a flow injection system at the molecular level. Results show that 2,4-D is a competitive inhibitor of catalase with an inhibition constant of 4.78×10^{-7} M. This work provides a method to evaluate the toxicity of 2,4-D and detecting 2,4-D quickly and sensitively. The application of this method can greatly simplify the testing process, shorten the operation time, and reduce the cost. It can be used for future study of the interaction between biomolecules and small molecules.

ASSOCIATED CONTENT

Supporting Information

The Supporting Information is available free of charge on the ACS Publications website at DOI: 10.1021/acs.jpcc.5b12559.

Scheme S1: Illustration of the inhibition mechanism of 2,4-D to catalase and the structure of 2,4-D (PDF)

AUTHOR INFORMATION

Corresponding Authors

*Tel: +86 514 87975568; Fax: +86 514 87975244; E-mail: xuqin@yzu.edu.cn.

*E-mail: xyhu@yzu.edu.cn.

Author Contributions

The manuscript was written through contributions of all authors. All authors have given approval to the final version of the manuscript.

Notes

The authors declare no competing financial interest.

ACKNOWLEDGMENTS

The authors gratefully acknowledge NSFC (21275124, 21275125, and 21575124), the Foundation of Yangzhou Environmental Protection Bureau (YHK1410), Open Project of State Key Laboratory of Analytical Chemistry for Life Science (SKLACLS1414), the high-end talent project of Yangzhou University, the project funded by the PAPD, and The Testing Center of Yangzhou University for the characterization data.

REFERENCES

(1) Mittler, R.; Vanderauwera, S.; Gollery, M.; Van Breusegem, F. Reactive oxygen gene network of plant. *Trends Plant Sci.* **2004**, *9*, 490−498.

(2) Willekens, H.; Chamnongpol, S.; Davey, M.; Schraudner, M.; Langebartels, C.; Montagu, M. V.; Inzé, D.; Van Camp, W. Catalase is

DOI: 10.1021/acs.jpcc.5b12559
J. Phys. Chem. C 2016, 120, 15966−15975

a sink for H_2O_2 and is indispensable for stress defence in C3 plants. *EMBO J.* **1997**, *16*, 4806−4816.
(3) Shim, I.; Naruse, Y.; Kim, Y. H.; Kobayashi, K.; Usui, K. Scavenging activity of NaCl-induced activated oxygen in two rice (Oryza sativa L.) cultivars differing in salt tolerance. *Jpn. J. Trop. Agr.* **1999**, *43*, 32−41.
(4) Monteiro, T.; Rodrigues, P. R.; Goncalves, A. L.; Moura, J. J. G.; Jubete, E.; Anorga, L.; Piknova, B.; Schechter, A. N.; Silveira, C. M.; Almeida, M. G. Construction of effective disposable biosensors for point of care testing of nitrite. *Talanta* **2015**, *142*, 246−251.
(5) (a) Zhang, H. X.; Ding, J. W.; Du, D. Electrochemical evaluation of the mechanism of acetylcholinesterase inhibition based on an electrodeposited thin film. *Int. J. Electrochem. Sci.* **2015**, *10*, 1632−1645. (b) Arduini, F.; Amine, A.; Moscone, D.; Palleschi, G. Reversible enzyme inhibition-based biosensors: applications and analytical improvement through diagnostic inhibition. *Anal. Lett.* **2009**, *42*, 1258−1293.
(6) The Industry Task Force II on 2,4-D Research Data, www.24d.org
(7) Bukowska, B. Toxicity of 2,4-dichlorophenoxyacetic acid-molecular mechanisms. *Pol. J. Environ. Stud.* **2006**, *15*, 365−374.
(8) Romero-Puertas, M. C.; Mccarthy, I.; Gómez, M.; Sandalio, L. M.; Corpas, F. J.; Del Rio, L. A.; Palma, J. M. Reactive oxygen species-mediated enzymatic systems involved in the oxidative action of 2,4-dichlorophenoxyacetic acid. *Plant, Cell Environ.* **2004**, *27*, 1135−1148.
(9) Wort, D. J.; Cowie, L. M. The effect of 2,4-dichlorophenoxyacetic acid on phosphorylase, phosphatase, amylase, catalase, and peroxidase activity in wheat. *Plant Physiol.* **1953**, *28*, 135−139.
(10) Mittler, R.; Vanderauwera, S.; Gollery, M.; Van Breusegem, F. Reactive oxygen gene network of plant. *Trends Plant Sci.* **2004**, *9*, 490−498.
(11) (a) Zhang, B.; Zhai, W.; Liu, R.; Yu, Z.; Shen, H.; Hu, X. Evaluation on the Toxic Effects of NanoAg to Catalase. *J. Nanosci. Nanotechnol.* **2015**, *15*, 1473−1479. (b) Teng, Y.; Zhang, H.; Liu, R. Molecular interaction between 4-aminoantipyrine and catalase reveals a potentially toxic mechanism of the drug. *Mol. BioSyst.* **2011**, *7*, 3157−3163. (c) Xu, Q.; Lu, Y.; Jing, L.; Cai, L.; Zhu, X.; Xie, J.; Hu, X. Specific binding and inhibition of 6-benzylaminopurine to catalase: multiple spectroscopic methods combined with molecular docking study. *Spectrochim. Acta, Part A* **2014**, *123*, 327−335.
(12) Shao, Q.; Wu, P.; Gu, P.; Xu, X.; Zhang, H.; Cai, C. Electrochemical and spectroscopic studies on the conformational structure of hemoglobin assembled on gold nanoparticles. *J. Phys. Chem. B* **2011**, *115*, 8627−8637.
(13) Ovalle, M.; Stoytcheva, M.; Zlatev, R.; Valdez, B. Electrochemical study of rat brain acetylcholinesterase inhibition by chlorofos: kinetic aspects and analytical applications. *Electrochim. Acta* **2009**, *55*, 516.
(14) Limoges, B.; Savéant, J.-M.; Yazidi, D. Quantitative analysis of catalysis and inhibition at horseradish peroxidase monolayers immobilized on an electrode surface. *J. Am. Chem. Soc.* **2003**, *125*, 9192−9203.
(15) (a) Wang, K.; Li, H. N.; Wu, J.; Ju, C.; Yan, J. J.; Liu, Q.; Qiu, B. TiO_2-decorated graphene nanohybrids for fabricating an amperometric acetylcholinesterase biosensor. *Analyst* **2011**, *136*, 3349−3354. (b) Li, D.; He, Q.; Cui, Y.; Duan, L.; Li, J. Immobilization of glucose oxidase onto gold nanoparticles with enhanced thermostability. *Biochem. Biophys. Res. Commun.* **2007**, *355*, 488−93.
(16) Gai, P. P.; Song, R. B.; Zhu, C.; Ji, Y. S.; Chen, Y.; Zhang, J. R.; Zhu, J. J. A ternary hybrid of carbon nanotubes/graphitic carbon nitride nanosheets/gold nanoparticles used as robust substrate electrodes in enzyme biofuel cells. *Chem. Commun.* **2015**, *51*, 14735−14738.
(17) Lin, K.; Wu, C.; Chang, J. Advances in synthesis of calcium phosphate crystals with controlled size and shape. *Acta Biomater.* **2014**, *10*, 4071−102.
(18) (a) Wang, H. S.; Wang, G. X.; Pan, Q. X. Electrochemical study of the interactions of DNA with redox-active molecules based on the immobilization of dsDNA on the sol-gel derived nano porous hydroxyapatite-polyvinyl alcohol hybrid material coating. *Electroanalysis* **2005**, *17*, 1854−1860. (b) Lucas, A.; Gaude, J.; Carel, C.; Michel, J. F.; Cathelineau, G. A synthetic aragonite-based ceramic as a bone graft substitute and substrate for antibiotics. *Int. J. Inorg. Mater.* **2001**, *3*, 87−94.
(19) Zhang, H.; Xu, J. J.; Chen, H. Y. One-step biomimetic coprecipitation method to form calcium phosphate and hemoglobin composite nanoparticles for biosensing application. *J. Electroanal. Chem.* **2008**, *624*, 79−83.
(20) Sun, Q.; Dai, Z.; Meng, X.; Xiao, F. Porous polymer catalysts with hierarchical structures. *Chem. Soc. Rev.* **2015**, *44*, 6018−6034.
(21) Xu, Q.; Cai, L.; Zhao, H.; Tang, J.; Shen, Y.; Hu, X.; Zeng, H. Forchlorfenuron detection based on its inhibitory effect towards catalase immobilized on boron nitride substrate. *Biosens. Bioelectron.* **2015**, *63*, 294−300.
(22) Xu, Q.; Jin, L.; Cai, L.; Yang, Z.; Hu, X. Direct electrochemistry of horseradish peroxidase based on hierarchical porous calcium phosphate microspheres. *Microchim. Acta* **2014**, *181*, 511−518.
(23) Lineweaver, H.; Burk, D. The determination of enzyme dissociation constants. *J. Am. Chem. Soc.* **1934**, *56*, 658−666.
(24) Xu, Q.; Lu, G.-j.; Bian, X.-J.; Jin, G.-d.; Wang, W.; Hu, X.-Y.; Wang, Y.; Yang, Z. Calcium phosphate−gold nanoparticles nanocomposite for protein adsorption and mediator-free H_2O_2 biosensor construction. *Mater. Sci. Eng., C* **2012**, *32*, 470−477.
(25) Varma, S.; Mattiasson, B. Amperometric biosensor for the detection of hydrogen peroxide using catalase modified electrodes in polyacrylamide. *J. Biotechnol.* **2005**, *119*, 172−80.
(26) Wang, Y.; Feng, J.; Tan, Z.; Wang, H. Electrochemical impedance spectroscopy aptasensor for ultrasensitive detection of adenosine with dual backfillers. *Biosens. Bioelectron.* **2014**, *60*, 218−223.
(27) Takahashi, T.; Tanase, S.; Yamamoto, Y. Electrical conductivity of some hydroxyapatites. *Electrochim. Acta* **1978**, *23*, 369−373.
(28) Huang, K.-J.; Niu, D.-J.; Liu, X.; Wu, Z.-W.; Fan, Y.; Chang, Y.-F.; Wu, Y.-Y. Direct electrochemistry of catalase at amine-functionalized graphene/gold nanoparticles composite film for hydrogen peroxide sensor. *Electrochim. Acta* **2011**, *56*, 2947−2953.
(29) Jia, W. Z.; Guo, M.; Zheng, Z.; Yu, T.; Rodriguez, E. G.; Wang, Y.; Lei, Y. Electrocatalytic oxidation and reduction of H_2O_2 on vertically aligned Co_3O_4 nanowalls electrode: Toward H_2O_2 detection. *J. Electroanal. Chem.* **2009**, *625*, 27−32.
(30) Arduini, F.; Errico, I.; Amine, A.; Micheli, L.; Palleschi, G.; Moscone, D. Enzymatic spectrophotometric method for aflatoxin B detection based on acetylcholinesterase inhibition. *Anal. Chem.* **2007**, *79*, 3409−3415.
(31) Şenay, A. C.; Öztop, H. N. Immobilization of catalase on chitosan film. *Enzyme Microb. Technol.* **2000**, *26*, 497.
(32) Marangoni, A. G. *Enzyme Kinetics: A Modern Approach*; John Wiley & Sons: Hoboken, NJ, 2002.
(33) Dixon, M. The determination of enzyme inhibitor constants. *Biochem. J.* **1953**, *55*, 170−171.
(34) Cornish-Bowden, A. A simple graphical method for determining the inhibition constants of mixed, uncompetitive and non-competitive inhibitors. *Biochem. J.* **1974**, *137*, 143−144.
(35) Ghica, M. E.; Brett, C. M. A. Glucose oxidase inhibition in poly(neutral red) mediated enzyme biosensors for heavy metal determination. *Microchim. Acta* **2008**, *163*, 185−193.
(36) Nikolelis, D. P. *Biosensors for Direct Monitoring of Environmental Pollutants in Field*; Nikolelis, D. P., Krull, U. J., Wang, J., Mascini, M., Eds.; Kluwer Academic Publishers: Dordrecht/Boston/London, 1997.
(37) Acker, M. G.; Auld, D. S. Considerations for the design and reporting of enzyme assays in high-throughput screening applications. *Perspect. Sci.* **2014**, *1*, 56−73.
(38) Costa, S. Z.; Tzanov, T.; Filipa Carneiro, A.; Paar, A.; Gubitz, G. M.; Cavaco-Paulo, A. Studies of stabilization of native catalase using additives. *Enzyme Microb. Technol.* **2002**, *30*, 387−391.
(39) Ruzicka, J. E.; Hansen, H. Flow injection analysis. Part I. A new concept of fast continuous flow analysis. *Anal. Chim. Acta* **1975**, *78*, 145−157.

DOI: 10.1021/acs.jpcc.5b12559
J. Phys. Chem. C 2016, 120, 15966−15975

(40) Gobi, K. V.; Kim, S. J.; Tanaka, H.; Shoyama, Y.; Miura, N. Novel surface plasmon resonance (SPR) immunosensor based on monomolecular layer of physically-adsorbed ovalbumin conjugate for detection of 2,4-dichlorophenoxyacetic acid and atomic force microscopy study. *Sens. Actuators, B* **2007**, *123*, 583−593.
(41) de Amarante, O. P., Jr.; Brito, N. M.; dos Santos, T. C. R.; Nunes, G. S.; Ribeiro, M. L. Determination of 2,4-dichlorophenoxyacetic acid and its major transformation product in soil samples by liquid chromatographic analysis. *Talanta* **2003**, *60*, 115−121.
(42) Xie, C.; Gao, S.; Guo, Q.; Xu, K. Electrochemical sensor for 2,4-dichlorophenoxy acetic acid using molecularly imprinted polypyrrole membrane as recognition element. *Microchim. Acta* **2010**, *169*, 145−152.
(43) (a) Wang, X.; Liu, X.; Wang, X. Surface-relief-gratings based on molecularly imprinted polymer for 2,4-dichlorophenoxyacetic acid detection. *Sens. Actuators, B* **2015**, *220*, 873−879. (b) Boro, R. C.; Kaushal, J.; Nangia, Y.; Wangoo, N.; Bhasin, A.; Suri, C. R. Gold nanoparticles catalyzed chemiluminescence immunoassay for detection of herbicide 2,4-dichlorophenoxyacetic acid. *Analyst* **2011**, *136*, 2125−2130. (c) Ding, J. H.; Lu, Z.; Wang, R. Z.; Shen, G. L.; Xiao, L. T. Piezoelectric immunosensor with gold nanoparticles enhanced competitive immunoreaction technique for 2,4-dichlorophenoxyacetic acid quantification. *Sens. Actuators, B* **2014**, *193*, 568−573.
(44) Vdovenko, M. M.; Stepanova, A. S.; Eremin, S. A.; Van Cuong, N.; Uskova, N. A.; Yu Sakharov, I. Quantification of 2,4-dichlorophenoxyacetic acid in oranges and mandarins by chemiluminescent ELISA. *Food Chem.* **2013**, *141*, 865−868.
(45) Shi, H.; Zhao, G.; Liu, M.; Zhu, Z. A novel photoelectrochemical sensor based on molecularly imprinted polymer modified TiO_2 nanotubes and its highly selective detection of 2,4-dichlorophenoxyacetic acid. *Electrochem. Commun.* **2011**, *13* (12), 1404−1407.
(46) Peng, D.; Li, X.; Zhang, L.; Gong, J. Novel visible-light-responsive photoelectrochemical sensor of 2,4-dichlorophenoxyacetic acid using molecularly imprinted polymer/BiOI nanoflake arrays. *Electrochem. Commun.* **2014**, *47*, 9−12.
(47) (a) Amine, A.; Mohammadi, H.; Bourais, I.; Palleschi, G. Enzyme inhibition basedbiosensors for food safety and environmental monitoring. *Biosens. Bioelectron.* **2006**, *21*, 1405−1423. (b) Amine, A.; Arduini, F.; Moscone, D.; Palleschi, G. Recent advances in biosensors based on enzyme inhibition. *Biosens. Bioelectron.* **2016**, *76*, 180−194.

DOI: 10.1021/acs.jpcc.5b12559
J. Phys. Chem. C 2016, 120, 15966−15975